J Mater Sci (2012) 47:473–478
DOI 10.1007/s10853-011-5822-z

Continuous high-pressure torsion using wires

Kaveh Edalati · Seungwon Lee · Zenji Horita

Received: 1 July 2011 / Accepted: 25 July 2011 / Published online: 6 August 2011

Abstract A newly developed severe plastic deformation method, continuous high-pressure torsion (CHPT), was modified for continuous processing of metallic wires. In this study, using the CHPT, wires of high-purity aluminum (99.99%) and copper (99.999%) with diameters of 2 mm and total lengths of 100 mm were successfully processed by employing the same features as conventional high-pressure torsion (HPT) technique. The results of hardness measurements, 35 Hv for Al and 116 Hv for Cu, after CHPT at an imposed equivalent strain of $\sim$13 were consistent with those of conventional HPT using disk and ring specimens, as well as with those of CHPT using sheet specimens. Transmission electron microscopy (TEM) demonstrated that the microstructural elements are elongated in the shear direction after CHPT. The average grain size reaches the steady-state level, $\sim$1.3 μm, in Al, but the microstructure is at the non-steady state in Cu with subgrain sizes in the range of 0.3–4 μm.

Introduction

Ultrafine-grained (UFG) microstructures and resultant high strength and reasonable ductility are achieved by processing materials through the application of high-pressure torsion (HPT) [1–4]. In the HPT method, a thin disk or ring is held between two anvils under a high pressure, and severe plastic deformation (SPD) is imparted by rotating the two anvils with respect to each other [5–7]. The HPT method has two main merits when compared with other severe plastic deformation (SPD) techniques. The first merit of HPT is the continuous-straining feature of the method and thus, it is effective to introduce giant shear strains up to a steady-state level [8–16]. On the contrary, other SPD methods, such as equal-channel angular pressing (ECAP), are noncontinuous in straining, and the workpiece should be subjected to several repetitive passes to attain high strains [17–22]. As a second merit of HPT, since the process is conducted under high hydrostatic pressures, the fracture of workpiece is significantly suppressed and thus, it is applicable to all kinds of metals and semi-metals [23] even including hard and less-ductile intermetallics and ceramics such as Ni_3Al [24] and Al_2O_3 [25].

Despite the merits with HPT, the use of the technique in industrial applications is limited because of the small dimensions of samples, although the sample size is currently extended to 40 mm in diameter for disks [26, 27] and 100 mm in diameter for rings [28]. The HPT process has been used in the form of disk or ring, but it is strongly desired to be performed in the form of sheet or wire. An alternative technique, continuous high-pressure torsion (CHPT) [29], was recently developed, which is applicable for the continuous processing of metallic sheets. The CHPT method should be effective in scaling up the sample size without sacrificing the pressure, whereas the sample size is limited in conventional HPT because the pressure is reduced with any increase in the sample size. The method of CHPT was conducted using the sheets of Al, Cu, and Fe with 0.6-mm thicknesses; 3-mm widths; and 40–80 mm lengths, and it could provide a continuous process for

K. Edalati (✉) · S. Lee · Z. Horita
Department of Materials Science and Engineering, Faculty of Engineering, Kyushu University, Fukuoka 819-0395, Japan
e-mail: kaveh.edalati@zaiko6.zaiko.kyushu-u.ac.jp

K. Edalati · S. Lee · Z. Horita
WPI, International Institute for Carbon–Neutral Energy Research (I2CNER), Kyushu University, Fukuoka 819-0395, Japan

obtaining a steady level of hardness and a minimum grain size in these metals [29].

In this study, in order to process metallic wires, which are more appropriate than disk and ring shapes for industrial applications, the CHPT using wire specimens is introduced with a simple modification of the earlier procedure for the CHPT using sheet specimens. Thus, taking advantage of the merits of CHPT, it is shown that wires of Al and Cu are processed in an expeditious way while maintaining the fundamental characteristics of HPT.

Principles and facilities

The principles of CHPT using sheet specimens were introduced in Ref. [29]. The facility for the CHPT using wires, schematically illustrated in Fig. 1, is similar to that for the CHPT using sheet specimens. The facility consists of two anvils: the lower anvil, which is rotated during process, has a roughened ring-shaped groove; and the upper anvil, which is fixed during process, has a half ring-shaped groove on the surface. The grooves have circular cross sections with 2-mm diameter, 0.9-mm depth, and outer diameter (OD) of 40 mm. A wire with 2-mm diameter is bent to a U-shape, as shown in Fig. 1, and it is used as an initial sample. Each sample is placed on the lower anvil, and the pressure is applied on the sample by raising the lower anvil to make a rigid contact with the upper anvil. The lower anvil is then rotated with respect to the upper anvil, and shear strain is introduced in the sample under a high pressure. Since the surface roughness of the groove on the upper anvil is intentionally reduced with respect to the surface roughness of the groove on the lower anvil, a continuous flow of the material occurs in the rotating direction because of the difference in slippage. The wire is also bent slightly upward and pulled out in tension manually during the process to maintain a continuous the material flow.

Figure 2 shows the appearance of the Al and Cu wires before and after CHPT for one revolution. It is apparent that the wires of Al and Cu with diameters of 2 mm and total lengths of 100 mm were successfully processed for the duration of 1 min using the CHPT. It should be noted that the wire is not round especially in the lower portion on the cross section after processing, but it is almost uniform along the longitudinal wire direction. Moreover, the cross section of the processed wire is decreased by $\sim 30\%$ when compared to that of the initial wire. Therefore, subsequent shaping processes such as wire drawing or round–concave rolling may be used for modifying the cross-sectional shape of the wire.

The equivalent strain imposed by CHPT, ε, is given as [29]

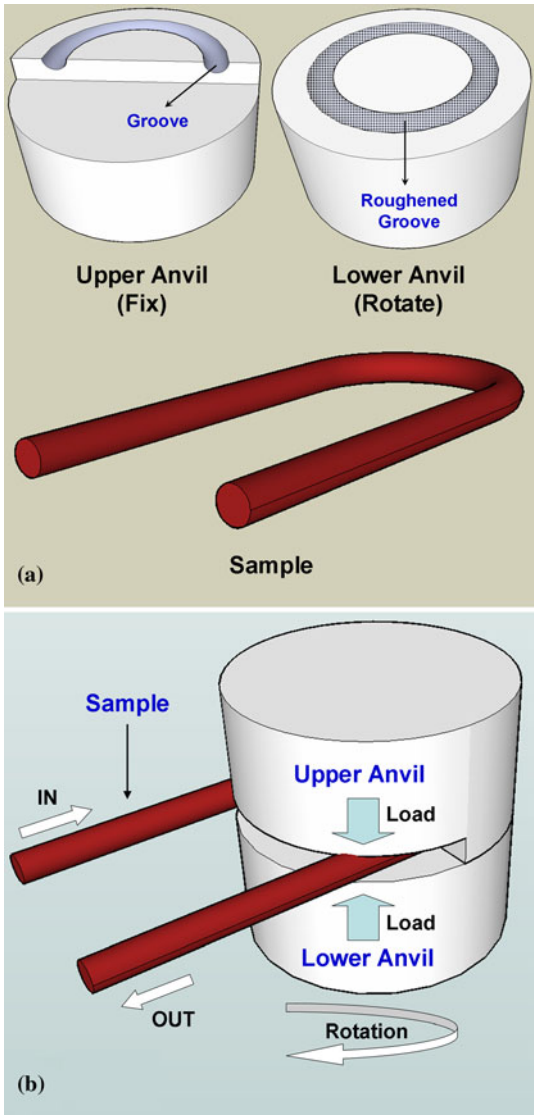

Fig. 1 Schematic illustration of CHPT using wire samples. Groove width: 2 mm, groove depth: 0.9 mm, outer diameter of groove: 40 mm, and wire diameter: 2 mm

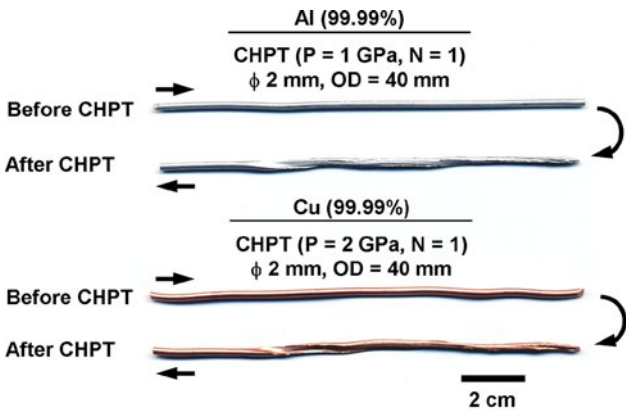

Fig. 2 Appearance of Al and Cu wires with 2-mm diameter before and after CHPT for one revolution

$$\varepsilon = (1 - s)\frac{\pi R}{\sqrt{3}t} \quad (1)$$

where, s is the fraction of sample slippage as described in an earlier study [30], R is the mean radius of the groove, and t is the sample thickness. For this study, R is 19.5 mm, t is 2 mm, and s is in the range of $0 < s < 1/2$ as estimated in Ref. [29]. It should be noted that $t = 2$ mm is the maximum value at the wire diameter but in practice, and it becomes smaller as the position is shifted away from the wire center. Since the real equivalent strain may scatter significantly from the nominal level because of the effect of slippage in proportion to $(1-s)$ [31], in this study, the equivalent strain was estimated under the condition of $s = 1/4 \pm 1/4$. The estimation leads to $\varepsilon = 13 \pm 4$ in this study.

Experimental materials and procedures

High-purity Al (99.99%) and Cu (99.99%) were received in the form of drawn wires with diameters of 2 mm for both Al and Cu, and lengths of 2 m (Al) and 5 m (Cu). These materials were selected because they matched the materials processed in earlier studies: HPT using disk [9, 32–35] and HPT using ring specimens [7, 28, 35]; CHPT using sheet specimens [29]; and ECAP using rod specimens [20–22], although the purity of Cu in this study is slightly higher than the 99.99% used in Refs. [32–35] and higher than the 99.96% used in Ref. [22]. The hardness values of wires in the drawn direction were 30 and 82 Hv for Al and Cu, respectively, which are similar to the hardness values of disk samples after the compression state of HPT [28, 35]. The wires were bent to U-shaped specimens, and each specimen was placed on the lower anvil. The pressures of 1 and 2 GPa were applied at room temperature on the Al and Cu specimens, respectively, by raising the lower anvil to make a rigid contact with the upper anvil. The lower anvil was then rotated with respect to the upper anvil with a rotation speed of 1.0 rpm until the rotation was terminated after one revolution. Following CHPT, the samples were evaluated in terms of Vickers microhardness and transmission electron microscopy (TEM).

For hardness measurement, disks, with 2 mm in diameter and 1 mm in thickness, were cut in the direction perpendicular to the longitudinal axis of the wire at positions 5 mm away from the exit of the upper anvil. The disk samples were then polished to a mirror-like surface, and the Vickers microhardness was measured along the radii from the disk center to periphery at 8 different radial directions with 0.4-mm increments. For each hardness measurement, loads of 50 g for Al and of 200 g for Cu were applied for 15 s. For TEM, rectangular strips with dimensions of $0.15 \times 2 \times 3$ mm^3, having a plane parallel to both the shear direction and the anvil surface, were prepared from the positions 5–8 mm away from the exit of the upper anvil. The strips were polished with an electrochemical polisher using a solution of 10% $HClO_4$, 20% $C_3H_8O_3$, and 70% C_2H_5OH for Al; and 15% HNO_3, 15% $C_3H_5(OH)_3$, and 70% CH_3OH for Cu. TEM was performed at an accelerating voltage of 200 kV for microstructural observation and for recording selected-area electron diffraction (SAED) patterns.

Results and discussion

Figure 3 plots the hardness variations across the cross section at the wire center as well as at the distances of 0.4 and 0.8 mm from the wire center for (a) Al and (b) Cu, respectively. The microhardness values remain reasonably at a constant level for each metal, suggesting that the homogeneity is established throughout the wire samples after CHPT. The average of hardness values across the cross section was taken for each metal and plotted in Fig. 4 together with earlier data of (a) Al and (b) Cu obtained by

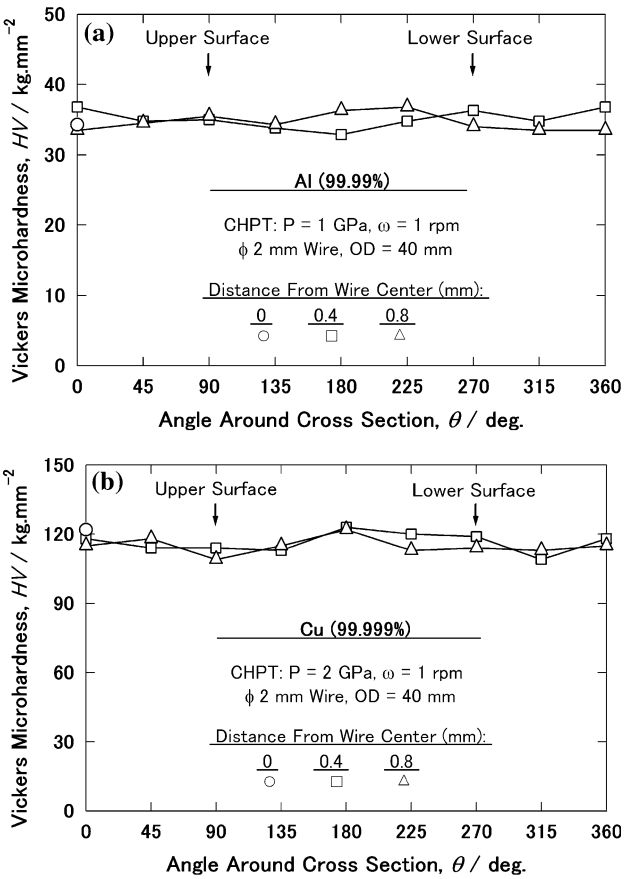

Fig. 3 Hardness variations across cross sections of **a** Al and **b** Cu wires after CHPT

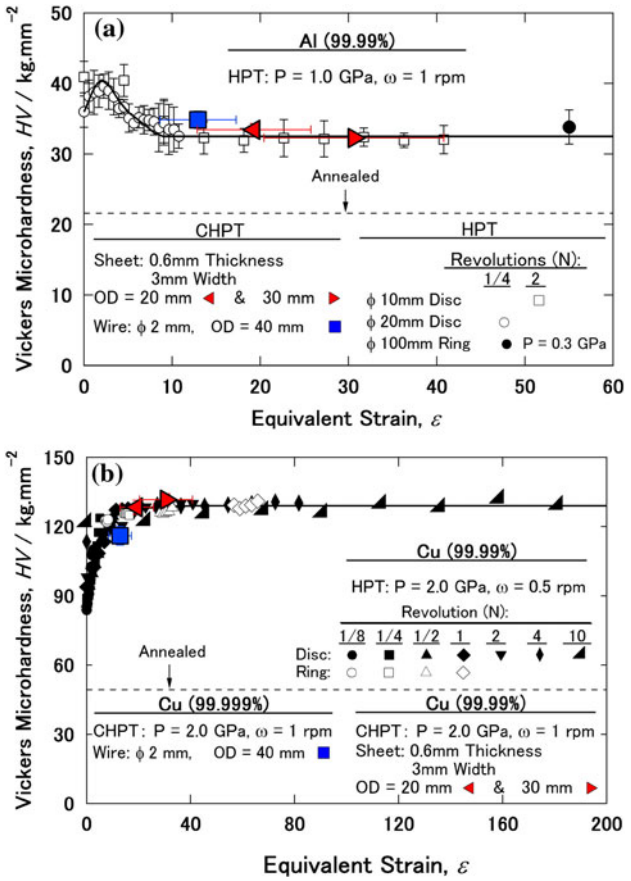

Fig. 4 Plots of Vickers microhardness against equivalent strain obtained earlier using conventional HPT for disk and ring samples of **a** Al [28] and **b** Cu [35] including results of CHPT using sheet [29] and wire samples

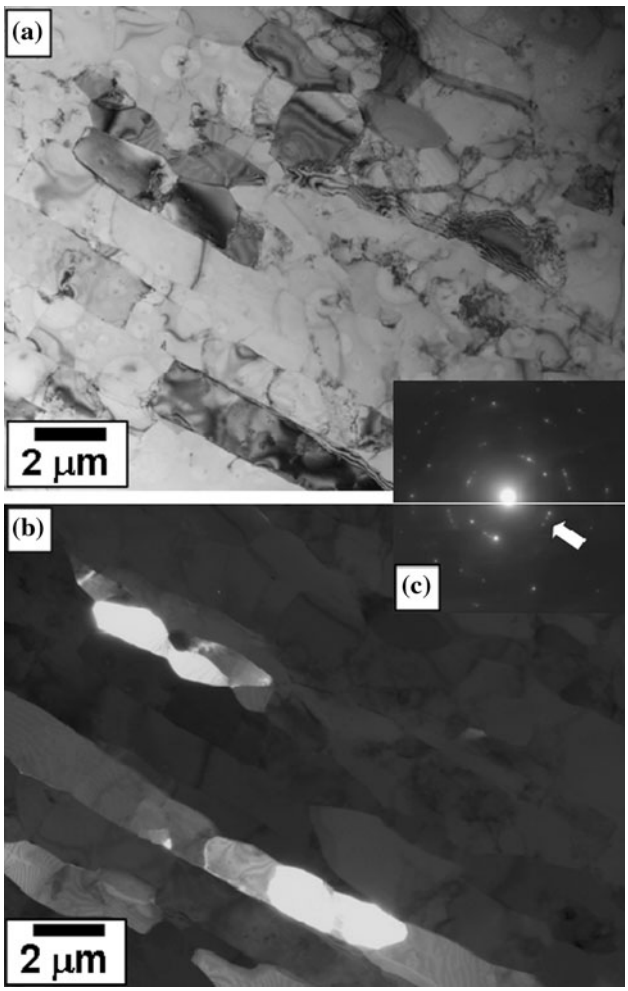

Fig. 5 TEM **a** bright-field and **b** dark-field micrographs including **c** SAED pattern of Al after processing with CHPT

conventional HPT using disk and ring specimens [28, 35]. In addition, the data obtained by CHPT using sheet specimens were taken from Ref. [29] and plotted in Fig. 4a and b. The results of HPT and CHPT are consistent except those of somewhat higher value obtained for Al wire processed with CHPT, and somewhat those of lower value obtained for Cu wire processed by CHPT. It should be noted that the present data were plotted applying $s = 1/4$, and this may result in overestimation of the equivalent strain ($\varepsilon = 13$ for wires). Inspection of Fig. 4a and b reveals that the imposed strain for the CHPT-processed Al wires remain almost on the steady state of straining, whereas the imposed strain for Cu wire is not enough to reach the steady state. It is noted that the steady state begins at equivalent strains of ~ 10 for Al [28] and of ~ 15 for Cu [35] using conventional HPT. In order to reach the steady level of hardness for Cu, the wire should be processed for a second pass through the anvils, or the ring diameter should be increased to 60–80 mm.

TEM microstructures are shown in Fig. 5 for the Al wire after CHPT processing, with a bright-field image and a dark-field image including the corresponding SAED pattern being shown in (a), (b) and (c). Note that the dark-field image was taken with the diffracted beam indicated by the arrow in the SAED pattern. It is apparent from Fig. 5 that few dislocations are visible in the grains, and that the grain boundaries are straight and well defined. These microstructural features, which are typical of grains after annealing, are consistent with the earlier observations using conventional HPT [7, 9, 35], CHPT with a sheet form of samples [29] and ECAP [20, 21]. However, inspection of Fig. 5a and b reveals that the grains are elongated in the rotating direction with an aspect ratio of 1.5 and with the average grain size of ~ 1.3 μm. These features of grains are different from the earlier observation using conventional HPT and CHPT with sheet samples, where the elongated grains were rarely seen within the microstructure. Two reasons may be considered for this difference: one is that the strain imparted in the sample was rather small as discussed in association with the higher hardness

shown in Fig. 4a, and the other may be due to the cross-sectional shape which is round for the wire sample. For the latter, the introduction of shear strain, and thus, the evolution of microstructure may be different from the one when using the thin disk and ring samples with an equal thickness.

TEM observations are summarized in Fig. 6 for Cu after CHPT, where (a) is a bright-field image, (b) is a dark-field image of (a) taken with the diffracted beam indicated by the arrow in the SAED pattern shown in (c). Inspection of this figure reveals that the microstructure consists of ill-defined subgrains, and that there are many dislocations within them. The average subgrain size appears to be in the range of 0.3–4 μm, and the misorientation angle should not be developed high, as evident from a discrete appearance of the diffractions spots in the SAED pattern. The average of subgrain size in Fig. 6 is larger than the averages of steady-state grain sizes of ~0.2 and ~ 0.27 μm reported for HPT- and ECAP-processed samples, respectively [22, 35]. However, the microstructural features observed in Fig. 6 are typical of microstructures at an early stage of straining by HPT and ECAP [22, 35]. As mentioned above, the imposed strain using the designed anvils is not high enough to reach the steady state in Cu.

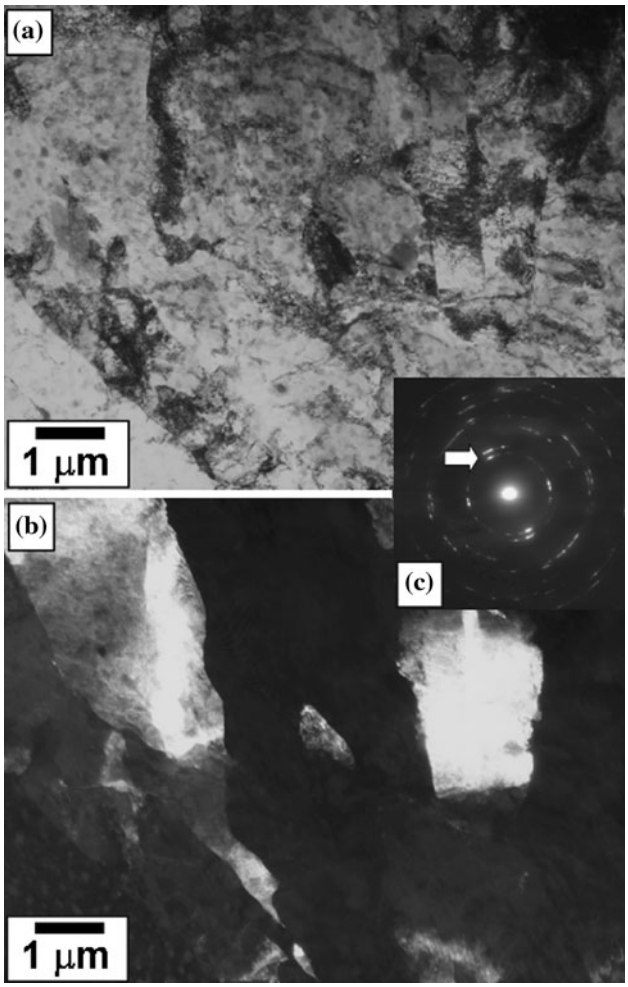

Fig. 6 TEM **a** bright-field and **b** dark-field micrographs including **c** SAED pattern of Cu after processing with CHPT

In summary, the method of CHPT can process long sizes of the wires in short time (100 mm per 1 min). Although there are over 20 continuous SPD techniques for producing wires [36], the CHPT is only the method that is feasible to reach a steady level of hardness and minimum grain size just after one pass through the anvils. However, the diameter of groove on the surface of anvils should be increased for processing the wires of harder metals such as Cu. It is noted that both the imposed strain and the processing speed are increased with an increase in the ring diameter.

Summary and conclusions

Continuous high-pressure torsion using wires was demonstrated in this article for microstructural refinement in metallic materials. Wires of high purity Al and Cu with 2-mm diameter and 100-mm length were successfully processed by continuous-torsional straining under high pressure using CHPT. The hardness and grain size reached a steady-state level for Al, but the imposed equivalent strain (13 ± 4) was not high enough to reach the steady state for Cu.

Acknowledgements One of the authors (KE) would like to thank the Islamic Development Bank (IDB) for a doctoral scholarship and Japan Society for Promotion of Science (JSPS) for a postdoctoral scholarship. This study was supported in part by the Light Metals Educational Foundation of Japan, in part by a Grant-in-Aid for Scientific Research from the MEXT, Japan, in Innovative Areas: "Bulk Nanostructured Metals," and in part by Kyushu University Interdisciplinary Programs in Education and Projects in Research Development (P&P).

References

1. Valiev RZ, Islamgaliev RK, Alexandrov IV (2000) Prog Mater Sci 45:103
2. Valiev RZ, Alexandrov IV, Zhu YT, Lowe TC (2002) J Mater Res 17:5
3. Valiev RZ, Estrin Y, Horita Z, Langdon TG, Zehetbauer MJ, Zhu YT (2006) J Oper Manage 58(4):33
4. Zhilyaev AP, Langdon TG (2008) Prog Mater Sci 53:893
5. Bridgman PW (1935) Phys Rev 48:825
6. Erbel S (1979) Met Technol 6:482
7. Harai Y, Ito Y, Horita Z (2008) Scripta Mater 58:469
8. Bonarski BJ, Schafler E, Mingler B, Skrotzki W, Mikulowski B, Zehetbauer MJ (2008) J Mater Sci 43:753. doi:10.1007/s10853-008-2794-8
9. Kawasaki M, Ahn B, Langdon TG (2010) J Mater Sci 45:4583. doi:10.1007/s10853-010-4420-9

10. Todaka Y, Umemoto M, Yamazaki A, Sasaki J, Tsuchiya K (2008) Mater Trans 49:47
11. Zhilyaev AP, Lee S, Nurislamova GV, Valiev RZ, Langdon TG (2001) Scripta Mater 44:2753
12. Hebesberger T, Stuwe HP, Vorhauer A, Wetscher F, Pippan R (2005) Acta Mater 53:393
13. Perez-Prado MT, Gimazov AA, Ruano OA, Kassner ME, Zhilyaev AP (2008) Scripta Mater 58:219
14. Wetscher F, Vorhauer A, Pippan R (2005) Mater Sci Eng A 410–411:213
15. Kilmametov AR, Khristoforova AV, Wilde G, Valiev RZ (2007) Z Kristallogr Suppl 26:339
16. Liao XZ, Zhao YH, Srinivasan SG, Zhu YT, Valiev RZ, Gunderov DV (2004) Appl Phys Lett 84:592
17. Segal VM, Reznikov VI, Drobyshevskiy AE, Kopylov VI (1981) Russian Metall 1:99
18. Valiev RZ, Langdon TG (2006) Prog Mater Sci 51:881
19. Valiev RZ, Langdon TG (2011) Metall Mater Trans A 528: 6140–6148
20. Iwahashi Y, Horita Z, Nemoto M, Langdon TG (1998) Acta Mater 46:3317
21. Kawasaki M, Horita Z, Langdon TG (2009) Mater Sci Eng A 524:143
22. Komura S, Horita Z, Nemoto M, Langdon TG (1999) J Mater Res 14:4044
23. Edalati K, Horita Z (2010) Scripta Mater 63:174
24. Rentenberger C, Waitz T, Karnthaler HP (2007) Mater Sci Eng A 462:283
25. Edalati K, Horita Z (2011) Scripta Mater 64:161
26. Pippan R, Scheriau S, Hohenwarter A, Hafok M (2008) Mater Sci Forum 584–586:6
27. Pippan R, Scheriau S, Taylor A, Hafok M, Hohenwarter A, Bachmaier A (2010) Annu Rev Mater Res 40:319
28. Edalati K, Horita Z (2009) Mater Trans 50:92
29. Edalati K, Horita Z (2010) J Mater Sci 45:4578. doi:10.1007/s10853-010-4381-z
30. Edalati K, Horita Z, Langdon TG (2009) Scripta Mater 60:9
31. Edalati K, Fujioka T, Horita Z (2009) Mater Trans 50:44
32. Xu C, Horita Z, Langdon TG (2007) Acta Mater 55:203
33. Kawasaki M, Figueiredo RB, Langdon TG (2011) Acta Mater 59:308
34. Edalati K, Ito Y, Suehiro K, Horita Z (2009) Int J Mater Res 100:1668
35. Edalati K, Fujioka T, Horita Z (2008) Mater Sci Eng A 497:168
36. Lowe TC (2011) Mater Sci Forum 667–669:1145